The Journal of Infectious Diseases

MAJOR ARTICLE

Multi-omics Based Identification of Specific Biochemical Changes Associated With PfKelch13-Mutant Artemisinin-Resistant *Plasmodium falciparum*

Ghizal Siddiqui, Anubhav Srivastava, Adrian S. Russell, and Darren J. Creek

Drug Delivery, Disposition and Dynamics, Monash Institute of Pharmaceutical Sciences, Monash University, Parkville, Victoria, Australia

Background. The emergence of artemisinin resistance in the malaria parasite *Plasmodium falciparum* poses a major threat to the control and elimination of malaria. Certain point mutations in the propeller domain of *PfKelch13* are associated with resistance, but *PfKelch13* mutations do not always result in clinical resistance. The underlying mechanisms associated with artemisinin resistance are poorly understood, and the impact of *PfKelch13* mutations on cellular biochemistry is not defined.

Methods. This study aimed to identify global biochemical differences between PfKelch13-mutant artemisinin-resistant and -sensitive strains of *P. falciparum* by combining liquid chromatography-mass spectrometry (LC-MS)-based proteomics, peptidomics, and metabolomics.

Results. Proteomics analysis found both *PfKelch13* mutations examined to be specifically associated with decreased abundance of PfKelch13 protein. Metabolomics analysis demonstrated accumulation of glutathione and its precursor, gamma-glutamylcysteine, and significant depletion of 1 other putative metabolite in resistant strains. Peptidomics analysis revealed lower abundance of several endogenous peptides derived from hemoglobin (HBα and HBβ) in the artemisinin-resistant strains.

Conclusion. *PfKelch13* mutations associated with artemisinin resistance lead to decreased abundance of PfKelch13 protein, decreased hemoglobin digestion, and enhanced glutathione production.

Keywords. malaria; *Plasmodium falciparum*; artemisinin resistance; PfKelch13; proteomics; metabolomics; peptidomics.

Malaria is a major global health problem, with >200 million cases of malaria and an estimated 429 000 deaths in 2015 [1]. *Plasmodium falciparum* causes the most severe form of malaria and is responsible for the highest incidence, especially in the World Health Organization African Region, where 90% of malaria cases and 92% of deaths due to malaria occur [1].

Artemisinin-based combination therapy (ACT) has been the recommended treatment for *P. falciparum* malaria since 2005 and has contributed to a significant reduction in malaria incidence and mortality [2]. However, the prevalence of ACT failure is increasing, especially in South-East Asia. Resistance to ACT was first reported in Western Cambodia and has now spread across the Greater Mekong Subregion, an area known historically for the emergence of resistance against previous first-line antimalarials [3]. The spread of chloroquine resistance from South-East Asia to Africa had significant implications for malaria control, and the emergence of artemisinin resistance in Africa could have devastating consequences.

Clinically, artemisinin resistance is defined by slow parasite clearance in *P. falciparum*–infected patients after treatment [3] and is associated with an increased survival of ring-stage parasites after short-term exposure to artemisinin in vitro [4, 5]. Recently, point mutations in the propeller domain of the *PfKelch13* gene (PF3D7_1343700) were shown to be associated with resistance to artemisinin in vitro and in vivo in South-East Asian *P. falciparum* strains [6–8]. To date, a total of 186 different *PfKelch13* alleles have been reported in Asia [9], but only a small subset of these mutants have been shown to be associated with artemisinin resistance [7, 8, 10–12], with 4 of these mutations (Y493H, R539T, I543T, and C580Y) further confirmed in vitro [6, 8, 13]. Furthermore, mutations in the *PfKelch13* gene have not yet been identified as associated with artemisinin resistance in African *P. falciparum* strains [14–19].

The use of *PfKelch13* as a genetic molecular marker for artemisinin resistance is time consuming and not always predictive of treatment outcome [9]. Additionally, labor-intensive in vitro assays are required for confirmation of resistance [19, 20]. An alternative set of biomarkers of artemisinin resistance would be valuable for epidemiological monitoring and potentially for point-of-care testing to assist with drug selection.

The genetic mutations responsible for artemisinin resistance likely mediate specific biochemical functions that help to define

Received 18 January 2017; editorial decision 6 March 2017; accepted 25 March 2017; published online March 27, 2017.

Presented in part: VIIN Young Investigator Symposium, Melbourne, Victoria, Australia, 14 October 2016. Abstract 31. American Society of Tropical Medicine and Hygiene Annual Meeting, Atlanta, Georgia, 14 November 2016.

Correspondence: D. J. Creek, PhD, Drug Delivery, Disposition and Dynamics, Monash Institute of Pharmaceutical Sciences, Monash University, Parkville Campus, Parkville, Victoria, Australia (darren.creek@monash.edu).

The Journal of Infectious Diseases® 2017;215:1435–44

DOI: 10.1093/infdis/jix156

the resistance phenotype [21]. In this study, differences in the biochemical phenotype of 3 pairs of *PfKelch13*-mutant parasites and relevant controls were characterized by analyzing their global proteome, metabolome, and peptidome.

This integrative multi-omics approach identified putative biomarkers that were consistently associated with artemisinin-resistant *PfKelch13* mutants, including the PfKelch13 protein, glutathione-related metabolites, and endogenous peptides derived from hemoglobin.

METHODS

Plasmodium falciparum Parasite Culture

All *P. falciparum* strains were cultured as previously described [22], and all analyses were performed within 6 weeks of the parasites being thawed. Parasites were tightly synchronized by double treatment with sorbitol, and when required, magnetic column purification was performed to obtain highly enriched trophozoite-stage infected red blood cells (RBCs) as described previously [23, 24]. The artemisinin-resistant and -sensitive *P. falciparum* isolates used in this study included 2 common *PfKelch13* mutants and the *PfKelch13* wild-type on an isogenic background [13] and 2 field strains [25] (Table 1). Global proteomic analyses were performed on ring- and trophozoite-stage parasites, but global metabolomics and peptidomics analyses were focussed only on trophozoite-stage parasites.

Global Proteomic Studies

Proteomics Sample Preparation

Intracellular parasites were purified from infected RBCs using 0.1% saponin as described previously [26]. Parasite pellets were solubilized with lysis buffer (100 mM N-2-hydroxyethylpiperazine-N-2-ethane sulfonic acid, 1% sodium deoxycholate, pH 8.1) supplemented with phosphatase and protease inhibitors for 5 minutes at 95°C. Proteins were reduced, alkylated, and then precipitated with trichloroacetic acid. The supernatants were kept for peptidomics sample preparation. The pellets were resuspended in 1 mL of lysis buffer, and then 500–800 µg of total protein (accurately determined using Pierce bicinchoninic acid (BCA) protein assay kit [Thermo Scientific Pierce]) were incubated overnight with trypsin (1:50; Promega). On the following day, dimethyl duplex labelling was performed [27]. After labelling, protein samples from the resistant and sensitive lines were mixed, and the peptide mixture was fractionated using a disposable Strong Cationic exchange solid-phase extraction cartridge (Agilent Bond Elut). Eluates and flowthrough (fractions) collected were subjected to desalting using in-house–generated StageTips as described previously [28]. The fractions were then dried and resuspended in 20 µL of 2% (v/v) acetonitrile and 0.1% (v/v) formic acid for liquid chromatography (LC)–mass spectrometry (MS)/MS analysis.

Proteomics Liquid Chromatography–Mass Spectrometry Analysis and Data Processing

Liquid chromatography–MS/MS was performed using an Ultimate U3000 Nano LC system (Dionex) and Q Exactive Hybrid Quadrupole-Orbitrap Mass Spectrometer (ThermoFisher). Samples were loaded at a high flow rate onto a reversed-phase trap column (100 µm × 2 cm) Acclaim PepMap media (Dionex) in 0.1% (v/v) formic acid in water. Peptides were eluted from the trap column at a flow rate of 0.3 µL/minute through a reversed-phase capillary column (75 µm × 15 cm; LC Packings, Dionex) into the nanospray ion source of the mass spectrometer. For proteomics analysis, the high-performance liquid chromatography gradient was set to 115 min using a gradient that reached 30% acetonitrile after 55 min, then 45% after 85 min, 55% after 90 min, and 90% after 100 min. The mass spectrometer was operated in data-dependent mode with 2 microscan fourier transform mass spectrometry scan events at 70 000 resolution (MS) over the *m/z* range of 375–1800 Da in positive-ion mode, and up to 20 data-dependent higher energy collision dissociation MS/MS scans.

Identification and quantification of proteins was performed using MaxQuant proteomics software [29]. Statistical analysis for the determination of differential proteins used parametric and nonparametric hypothesis testing and a linear model approach. Log-transformed fold-difference for paired artemisinin-resistant and -sensitive samples and one sample *t* test were calculated in Microsoft Excel to test the mean

Table 1. *Plasmodium falciparum* Strains Used

Strain name	Response to artemisinin (700 nM)[a]	*PfKelch13* genotype	Identifying description	Geographical source
Cam3.II^{rev}	0.7% survival using an in vitro $RSA_{0\text{-}3h}$	Wild-type	Cam3.II^{rev}, isogenic derivative of Cam3.II^{R539T}	Pursat Province, Cambodia [13]
Cam3.II^{R539T}	49% survival using an in vitro $RSA_{0\text{-}3h}$	R539T	Cam3.II^{R539T}, parent of Cam3.II^{rev} and Cam3.II^{C580Y}	
Cam3.II^{C580Y}	24% survival using an in vitro $RSA_{0\text{-}3h}$	C580Y	Cam3.II^{C580Y}, isogenic derivative of Cam3.II^{R539T}	
PL2	5% minimum viability using an in vitro RSA_{3h}	Wild-type	Pailin- PL2, field isolate (genetically distinct from PL7)	Western Cambodia [25]
PL7	20% minimum viability using an in vitro RSA_{3h}	R539T	Pailin- PL7, field isolate (genetically distinct from PL2)	

[a]Determined using in vitro ring-stage assay 0 to 3 hours/3 hours ($RSA_{0\text{-}3h}/RSA_{3h}$)

of combined experiment groups against the known mean (μ = 0) [30]. Bonferroni correction was applied to the significance threshold to adjust for multiple testing. Rank product analysis, a nonparametric permutation test, was conducted on the log-transformed fold-difference for paired artemisinin-resistant and -sensitive samples using the RankProd R package [31]. The significance of each protein was assessed by the *P* value and false discovery rate. Limma analysis, a linear model designed to assess differential expression, was conducted using the limma R package [32]. The significance of each protein was assessed by the *P* value and adjusted *P* value (adjusted for multiple testing) calculated with the empirical Bayesian framework applied to the linear model.

Global Metabolomics Studies

Metabolomics Sample Preparation

Plasmodium falciparum parasites were synchronized using sorbitol 24 hours before parasite harvest for metabolomics experiments. A control culture containing only uninfected RBCs was also analyzed. Metabolites were extracted from magnetically enriched parasites (5×10^7) at 60%–70% parasitaemia using cold methanol as previously described [33]. Insoluble precipitates were removed by centrifugation, and 100 μL of metabolite extract were transferred to glass liquid chromatography-mass spectrometry (LC-MS) vials and stored at −20°C until analysis. An aliquot (20 μL) of each sample was combined to generate a pooled biological sample for quality control procedures.

Metabolomics Liquid Chromatography–Mass Spectrometry Analysis and Data Processing

Hydrophilic interaction LC (ZIC-pHILIC, Merck) coupled with high-resolution MS (Q Exactive, ThermoFisher) was used to analyze metabolomics samples as previously described [34]. Approximately 250 metabolite standards were analyzed immediately preceding the batch run to determine accurate retention times to facilitate metabolite identification. Additional retention times for metabolites lacking authentic standards were predicted computationally as previously described [35]. Identification and quantification of metabolites was performed using the IDEOM workflow [36], and peak areas for significant metabolites were confirmed by manual integration of raw LC-MS data with TraceFinder (ThermoFisher).

Liquid chromatography–MS peak heights, representing metabolite abundances, were normalized according to the median identified peak for each sample. Univariate statistical analysis was done using IDEOM and Welch's *t* test [36]. Multivariate statistical analysis used partial least squares–discriminant analysis and was applied to log-transformed and auto-scaled data using the Web-based analytical tool MetaboAnalyst [37].

Global Peptidomics Studies

Peptidomics Sample Preparation

Supernatants collected after trichloroacetic acid precipitation from proteomics sample preparations were subjected to centrifugal filtration (10 kDa cutoff, Amicon Ultra). The flow-through was collected, and an equal amount of ethyl acetate was added to remove residual sodium deoxycholate. Equal quantities of total peptides (50–70 μg measured using Pierce BCA protein assay kit) were then used for peptidomics analyses. Peptide samples were subjected to desalting [28] and were then dried and resuspended in 20 μL of 2% (v/v) acetonitrile and 0.1% (v/v) formic acid for LC-MS/MS analysis.

Peptidomics Liquid Chromatography–Mass Spectrometry Analysis and Data Processing

Liquid chromatography–MS/MS was performed using the same methodology as the proteomics LC-MS/MS analysis (described above and in Supplementary Methods) with minor modifications. Mass identification with +1 and up to +8 charge was also enabled.

Peptide identification was conducted with de novo sequencing–assisted database search using PEAKS DB software [38]. The identified peptide sequences from the *Homo sapiens* and *P. falciparum* proteome databases that were detected in multiple samples were shortlisted. The mass-to-charge ratio and retention time of 148 shortlisted peptides were imported into TraceFinder (ThermoFisher), and the peak intensity was obtained by manually adjusting the integration and accounting for retention time drift when required. Log-transformed fold-difference and Welch's *t* test were calculated in Microsoft Excel for paired artemisinin-resistant and -sensitive samples.

RESULTS

This study combined metabolomics, peptidomics, and proteomics (Figure 1) to identify novel potential biomarkers for *PfKelch13*-mutant *P. falciparum* isolates associated with artemisinin resistance. Resistant and sensitive *P. falciparum* parasite isolates (Table 1) were synchronized and grown in vitro to the equivalent stage of the intraerythrocytic cycle (rings: 6–12 hours after invasion; trophozoites: 24- 30 hours after invasion), followed by parallel extractions for metabolomics, peptidomics, and proteomics analysis by LC-MS (Figure 1).

Quantitative Dimethyl-Based Proteomic Analysis

Global proteome analysis was performed using reductive dimethyl labeling to identify quantitative differences in protein levels between artemisinin-sensitive and -resistant *P. falciparum* isolates. Two clonal artemisinin-resistant isolates with defined *PfKelch13* mutations (Cam3.II^{R539T} and Cam3.II^{C580Y}) were compared with their isogenic *PfKelch13* wild-type strain (Cam3.II^{rev}) [13], and 2 independent field isolates from the Pailin region of Cambodia—a *PfKelch13*-mutant artemisinin-resistant

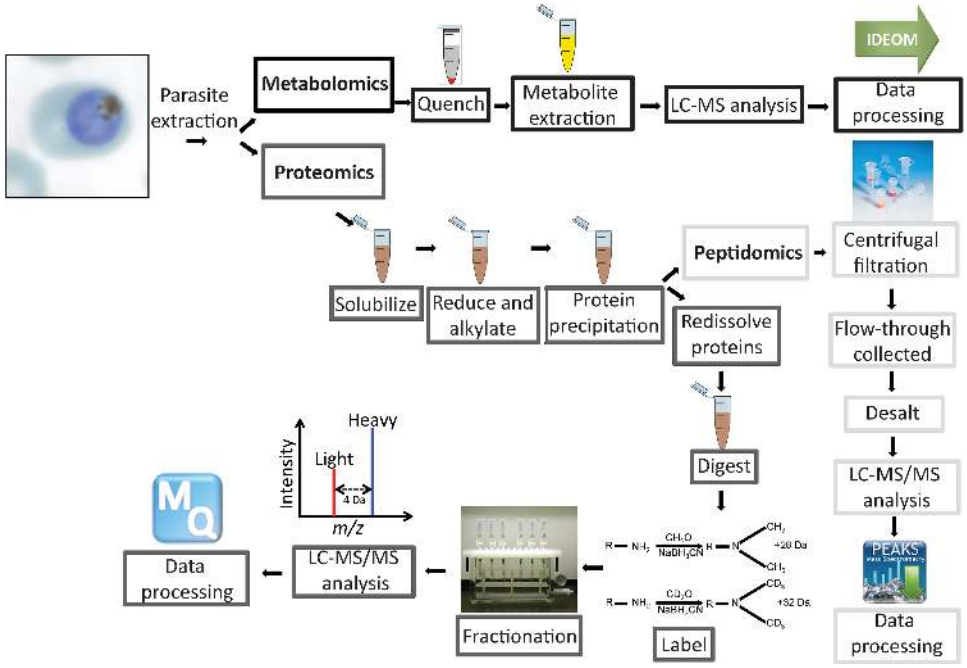

Figure 1. Flow chart of the integrative multi-omics approach (metabolomics, proteomics, and peptidomics) used for the analysis of *Plasmodium falciparum*–infected red blood cells (iRBCs). For metabolomics (indicated in black boxes), an equal number of cells (5×10^7) were used for metabolite extractions, samples were analyzed using liquid chromatography–mass spectrometry (LC-MS), and data were processed using IDEOM. For peptidomics (indicated in light gray boxes and arrows), an equal amount of peptides (50–70 µg) was used for analysis using LC-MS/MS, and data were processed and quantitatively analyzed using PEAKS. For proteomics (indicated in gray boxes), an equal amount of total protein (500–800 µg) was labeled using reductive dimethyl labeling for quantitative analysis. Samples from artemisinin-resistant and -sensitive iRBCs were then analyzed using LC-MS/MS, and the data were processed and analyzed using Maxquant. Abbreviations: LC, liquid chromatography; MS, mass spectrometry.

isolate (PL7) and *PfKelch13* wild-type sensitive (PL2) isolate [25]—were compared with each other (Table 1).

Saponin-lysed ring-stage parasite proteins from Cam3.II^{R539T} and Cam3.II^{rev} were labeled for quantitative proteomics from 3 biological replicates. Ring-stage parasites were chosen for initial proteomic analysis because this is the stage where differential in vitro sensitivity to artemisinin has been reported [6–8]. A total of 920 proteins were identified with at least 2 unique peptides, with 432 proteins in common between the 3 replicates (Supplementary Data File 1). Compared with the control, a significant reduction in the abundance of 6 proteins was observed ($P \leq .05$; log fold-change >0.5), including the PfKelch13 protein itself (Figure 2), and only 1 protein, Pf13_0341, a putative DNA-directed RNA polymerase 2, was significantly more abundant in the resistant strain (Supplementary Data File 1). It was noted that the ring-stage proteomics data demonstrated relatively poor coverage and high variability, likely due to the challenges associated with purification of ring-stage parasites following saponin lysis. Although decreased ring-stage sensitivity to artemisinins is the accepted in vitro model for artemisinin resistance, decreased sensitivity has also been reported for trophozoite stages when treated for a short duration (<2 hours) [25], suggesting that the resistance mechanism is not stage specific. Therefore, further studies were performed on trophozoite-stage parasites, allowing improved reproducibility and purity from uninfected RBC contaminants.

For trophozoite-stage parasites, 2824 proteins were identified from 3–4 biological replicates of 3 pairs of parasite strains (Supplementary Data File 1). Data from all 11 experiments were combined to detect significant proteins associated with all 3 resistant strains tested, and 3 types of statistical tests were applied to minimize the likelihood of false discoveries. Because

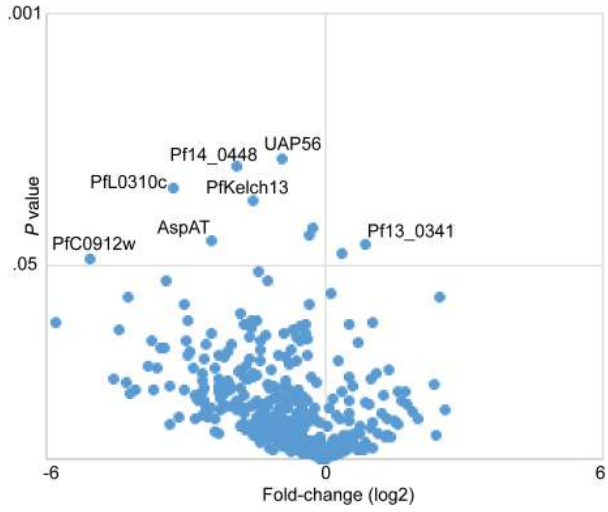

Figure 2. Volcano plot of ring-stage protein abundance in Cam3.II^{R539T} compared with Cam3.II^{rev}. Log_2 fold changes (*x*-axis) and *t* test *P* values (*y*-axis) of all proteins in ring-stage parasites (6–12 hours after invasion). Protein names are labeled next to significantly different proteins.

the rank product analysis performs poorly with datasets containing missing values, the dataset was restricted to proteins detected in all 11 experiments, resulting in a set of 520 proteins for analysis. The limma analysis was also conducted on an expanded data set of 1133 proteins that were detected in at least 1 experiment for each of the 3 pairs of parasite strains, and the same significant proteins were identified (data not shown). Only 5 proteins were apparently different ($P < .05$) according to each of the statistical tests applied (Table 2). However, when taking multiple testing corrections for all 3 tests into account (Bonferroni correction for *t* test, false discovery rate for rank product analysis, and adjusted *P* value for limma), only PfKelch13 abundance was found to be significantly different across all parasite strains (Table 2). PfKelch13 abundance was approximately 2-fold lower in the resistant strain across all 14 individual experiments including ring- and trophozoite-stage parasites (Figure 3A). The identification of PfKelch13 was confidently assigned based on the detection of 20 unique peptides, and manual analysis of the data confirmed lower abundance of peptides from both the N-terminal region and the C-terminal propeller domain in resistant (*PfKelch13*-mutant) compared with sensitive (wild-type) strains (Figure 3B).

Metabolomics Analysis of Artemisinin-Resistant Parasites

Comparative untargeted metabolomics was used to investigate the impact of resistance-associated *PfKelch13* mutations on the metabolome of 2 clonal resistant lines, Cam3.II^{R539T} and Cam3.II^{C580Y}, relative to the sensitive line, Cam3.II^{rev} (n = 3 biological replicates). Univariate statistical analysis of all identified metabolite features revealed few significant differences between the wild-type and both mutant lines. Supervised multivariate analysis (partial least squares–discriminant analysis) revealed a combination of metabolic features in the second component (PC2) that were associated with resistance (Figure 4A). Detailed analysis of this model revealed four metabolites with variable importance in projection scores >0.3, and subsequent manual integration of LC-MS data for these features confirmed that 1 metabolite was significantly depleted in the resistant lines and 3 were more abundant (Figure 4B). Levels of glutathione and its precursor gamma-glutamylcysteine were 74%, and 57% higher in the resistant parasites than the sensitive parasites, respectively. Levels of NAD^+ were only 20% higher in the resistant parasites than the sensitive parasites. The depleted metabolic feature in both resistant strains was putatively identified as L-proline amide. This metabolite was detected in the uninfected RBCs and is likely derived from the host cells (Supplementary Data File 2).

Peptidomics Analysis of Artemisinin-Resistant Parasites

Proteolysis is an important biochemical function in *P. falciparum*, and degradation of parasite (via the proteasome) and host (via the digestive vacuole) proteins has been proposed to influence the mechanism of action and/or resistance of artemisinin [39]. Most endogenous peptides liberated by protein digestion processes are not detected on the standard metabolomics and proteomics methods, necessitating the incorporation of a dedicated peptidomics analysis to investigate these proteolytic pathways. Peptidomics analysis identified 146 endogenous peptides that aligned with proteins from the *P. falciparum* (68 peptides) and *H. sapiens* (78 peptides) databases (Supplementary Data File 3). Significant reductions in the abundance of 19 peptides were observed in artemisinin-resistant lines compared with their appropriate controls ($P \leq .05$; log fold-change >0.5), including 8 peptides that originated from Hbβ, 10 that originated from Hbα (Figure 5), and 1 that originated from another *H. sapiens* protein, Uniprot ID number POU3F3 (Supplementary Data File 3). No significant differences in the abundance of *P. falciparum*–derived peptides were observed.

DISCUSSION

Integrative multi-omics approaches provide a comprehensive analysis of the abundance of cellular biochemicals, which can help in understanding the mechanism of artemisinin resistance. In this study, the proteomic, peptidomic, and metabolic profiles of artemisinin-resistant *P. falciparum* strains were investigated to reveal the biochemical impact of artemisinin resistance–associated *PfKelch13* mutations. The multi-omics analysis revealed that *PfKelch13* mutations do not have a widespread impact on the

Table 2. *Plasmodium falciparum* Proteins Differentially Regulated in Expression in Trophozoite-Stage Parasites of Artemisinin-Resistant (Cam3.II^{R539T}, Cam3.II^{C580Y}, PL7) Compared With Artemisinin-Sensitive (Cam3.II^{rev} and PL2) Lines

Uniprot/PlasmoDB ID	Protein	N	Relative abundance, mean ± SD	Student's *t* test P value	Limma *P* value	Rank product *P* value	Rank product FDR	Limma adjusted *P* value
Q8IDQ2/ PF3D7_1343700	PfKelch13 protein, putative	11	0.63 ± 0.09	2.63×10^{-6}[a]	1.1×10^{-5}	0	0	.006
Q8I492/ PF3D7_0500800	Mature parasite-infected erythrocyte surface antigen	11	0.81 ± 0.14	.002	.009	.02	.45	.78
Q8IIJ9/ PF3D7_1116700	Probable cathepsin C	11	0.81 ± 0.2	.02	.013	.04	.61	.78
Q6ZMA7/ PF3D7_0406200	Sexual stage–specific protein	11	2.0 ± 1.4	.02	.011	0	.01	.78
Q8IC42/ PF3D7_0702500	Uncharacterized protein	11	1.4 ± 0.5	.02	.03	.004	.12	.78

n = 11. PfKelch13 is the only protein significantly downregulated in artemisinin-resistant lines according to all three analyses after adjustment for multiple testing ($P < .05$).

[a]Less than Bonferroni-corrected *P* value threshold ($\alpha = 4.03 \times 10^{-5}$).

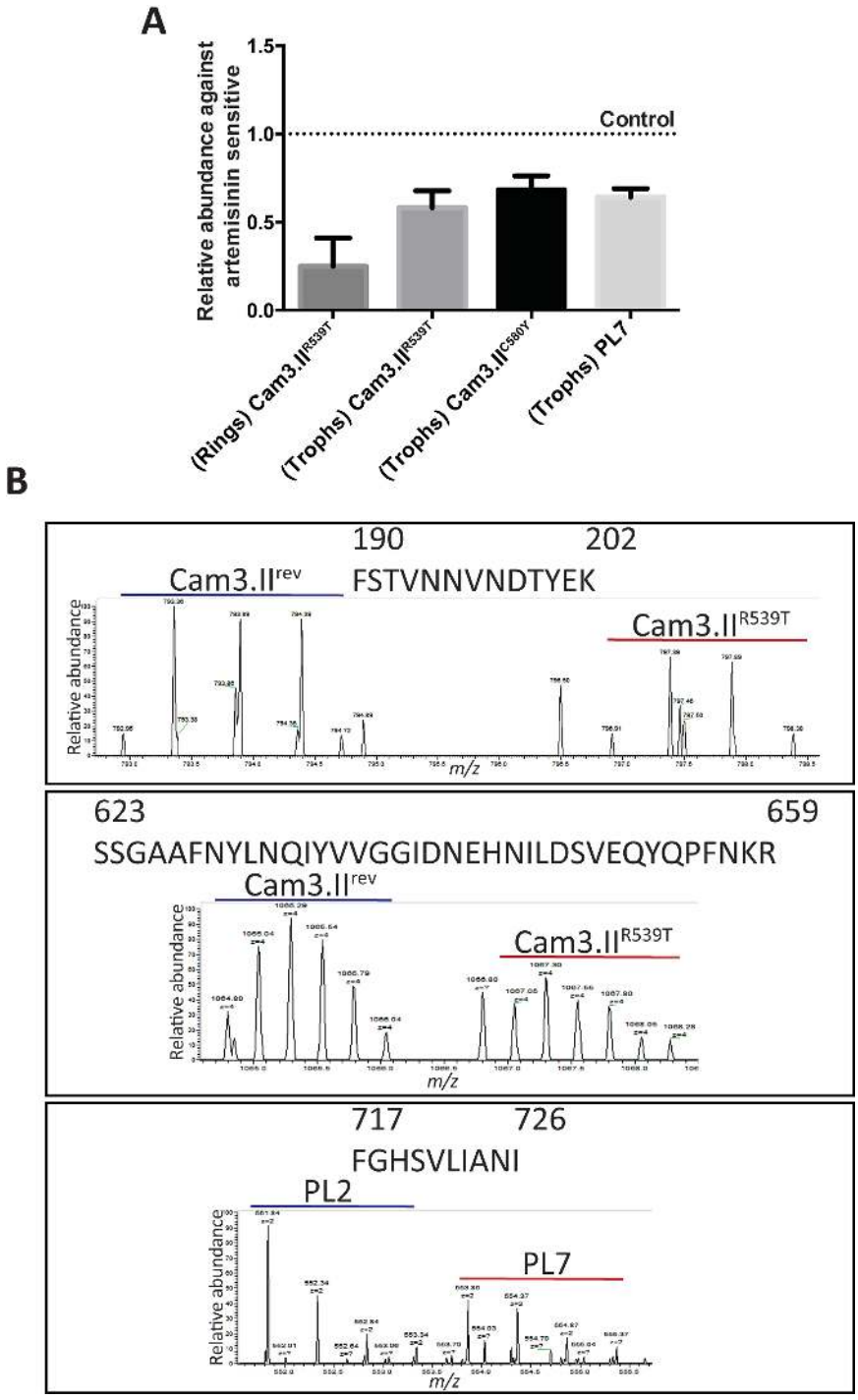

Figure 3. PfKelch13 is consistently and significantly downregulated in artemisinin-resistant lines compared with their relevant controls. *A,* Relative abundance (mean ± standard deviation) of PfKelch13 in 3 different artemisinin-resistant lines compared with their appropriate controls (see Table 1). *B,* Representative raw mass spectrometry spectra of tryptic peptides from a 1:1 mixture of Cam3.II^{R539T}/PL7 (heavy labeled) and control and Cam3.II^{rev}/PL2 (light labeled) extracts. The tryptic peptides (190-FSTVNNVNDTYEK-202, 623-SSGAAFNYLNQIYVVGGIDNEHNILDSVEQYQPFNKR-659, 717-FGHSVLIANI-726) belonging to N- and C-terminal regions of PfKelch13 show approximately 2-fold lower relative abundance for the heavy-labeled peptides compared with light-labeled peptides.

biochemistry of *P. falciparum* under standard in vitro culture conditions. The abundance of PfKelch13 protein itself was found to be consistently lower in all of the resistant lines compared with the sensitive strains. Endogenous peptides originating from hemoglobin and 1 putative host-derived metabolite were also decreased in abundance, whereas levels of glutathione and gamma-glutamylcysteine were higher in artemisinin-resistant lines compared with the *PfKelch13* wild-type, artemisinin-sensitive controls.

Artemisinin resistance is associated with point mutations on the *PfKelch13* allele. The exact function of PfKelch13 is not

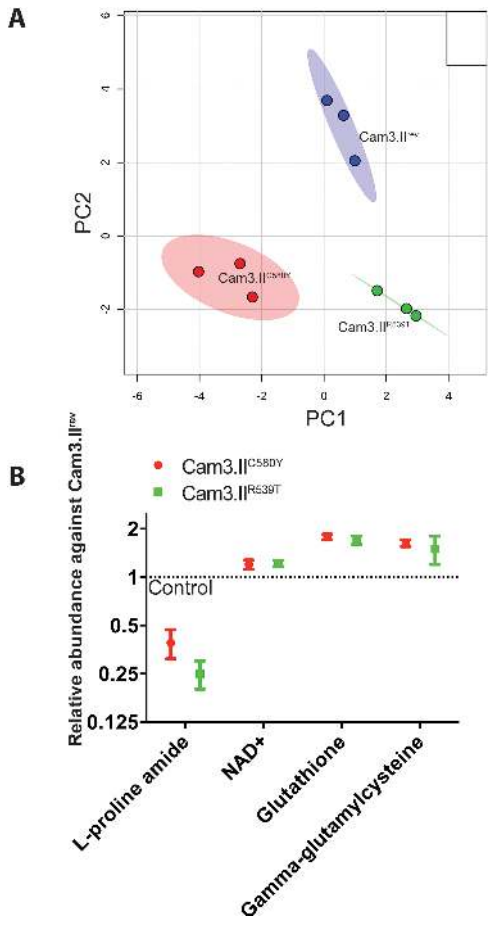

Figure 4. Differentially abundant metabolites in artemisinin-resistant (Cam3.II^{R539T} and Cam3.II^{C580Y}) versus artemisinin-sensitive (Cam3.II^{rev}) lines. *A,* Multivariate analysis (partial least squares–discriminant analysis) of all putative metabolite features detected in Cam3.II^{R539T}, Cam3.II^{C580Y}, and Cam3.II^{rev}. Sample projection (3 groups) onto the first partial least squares–discriminant analysis discriminant plane of Cam3.II^{rev}, Cam3.II^{R539T}, and Cam3.II^{C580Y}. *B,* Relative abundance of the 4 most differentially abundant metabolites from infected red blood cells in 2 artemisinin-resistant (Cam3.II^{R539T}, Cam3.II^{C580Y}) lines compared with the control (Cam3.II^{rev}). Data are presented as mean ± standard deviation (n = 3).

yet known; however, the C-terminal propeller domain shows homology to the human Keap1 protein, whose main function is to respond to oxidative stress by regulating levels of the transcription factor Nrf2 [6, 40]. Interestingly, the global proteomics analysis of ring and trophozoite parasite stages in both artemisinin-resistant laboratory-generated clonal lines and field isolates identified decreased abundance of PfKelch13 protein as the only significant differentiating feature (Figures 2 and 3; Table 2). Although no Nrf2 homologue has been identified in *P. falciparum*, based on Keap1 function, it is plausible that lower levels of PfKelch13 protein in artemisinin-resistant parasites would decrease the Kelch-mediated negative regulation of the stress response, thereby making parasites more resilient to drug-induced oxidative stress. The observed increase in glutathione abundance supports this hypothesis. It has also been hypothesized that the PfKelch13 protein is involved in the ubiquitination and proteasomal degradation of proteins within the endoplasmic reticulum and is involved in the correct folding of proteins within the parasite [39]. In this case, it is anticipated that depletion of PfKelch13 protein in artemisinin-resistant parasites would be associated with a dysregulated unfolded protein response, which is consistent with the previously reported increase in mRNA expression of genes associated with unfolded protein response [41], although no difference in abundance of those proteins was observed in the untreated in vitro conditions described here (Supplementary Data File 1).

Although the link between *PfKelch13* mutations and artemisinin resistance is well-established, *PfKelch13* expression was not previously associated with artemisinin resistance [41], suggesting that the differential protein abundance observed here may arise due to decreased translation or enhanced degradation of the PfKelch13 protein rather than transcriptional regulation. It has previously been demonstrated that artemisinin resistance in laboratory-generated *PfKelch13*^{C580Y}-mutant parasites (NF54 strain) is associated with an increased abundance of *P. falciparum* phosphatidylinositol-3-kinase (PfPI3K) and its lipid product phosphatidylinositol-3-phosphate (PI3P), likely due to a deficiency in PfKelch13-mediated, ubiquitin-dependent degradation of PfPI3K [42]. This hypothesis is consistent with the decreased abundance of PfKelch13 observed here, albeit these studies are based on parasites with different genetic backgrounds. Unfortunately, this untargeted metabolomics and proteomics approach was not capable of detecting PI3P and PfPI3K (Supplementary Data Files 1 and 2). Other published untargeted proteomics studies of blood-stage *P. falciparum* have also failed to detect peptides from PfPI3K in the absence of phosphopeptide enrichment [43]. Nevertheless, this study was able to successfully demonstrate the specific impact of 2 common *PfKelch13* mutations (C580Y and R539T) on PfKelch13 protein abundance and suggest that there is potential to develop a quantitative biomarker assay for artemisinin resistance that is independent of the specific *PfKelch13* genotype. Further studies on diverse *PfKelch13* genotypes are necessary to confirm the association between PfKelch13 protein abundance and clinical artemisinin resistance.

Although the *PfKelch13*-mutant parasites did not exhibit significant changes to the proteome (beyond PfKelch13) under these in vitro conditions, enhanced levels of glutathione and its precursor, gamma-glutamylcysteine, were observed in the metabolomics analysis. Glutathione is a cofactor required for detoxification enzymes such as glutathione peroxidase and glutathione S-transferase, and its abundance is suggestive of the parasite's ability to defend itself against additional oxidative stresses, such as that induced by artemisinin treatment [25, 44]. It has been proposed that artemisinin-resistant parasites are able to better manage oxidative damage [39], and increased glutathione concentration has been reported in rodent models of artemisinin resistance [45, 46].

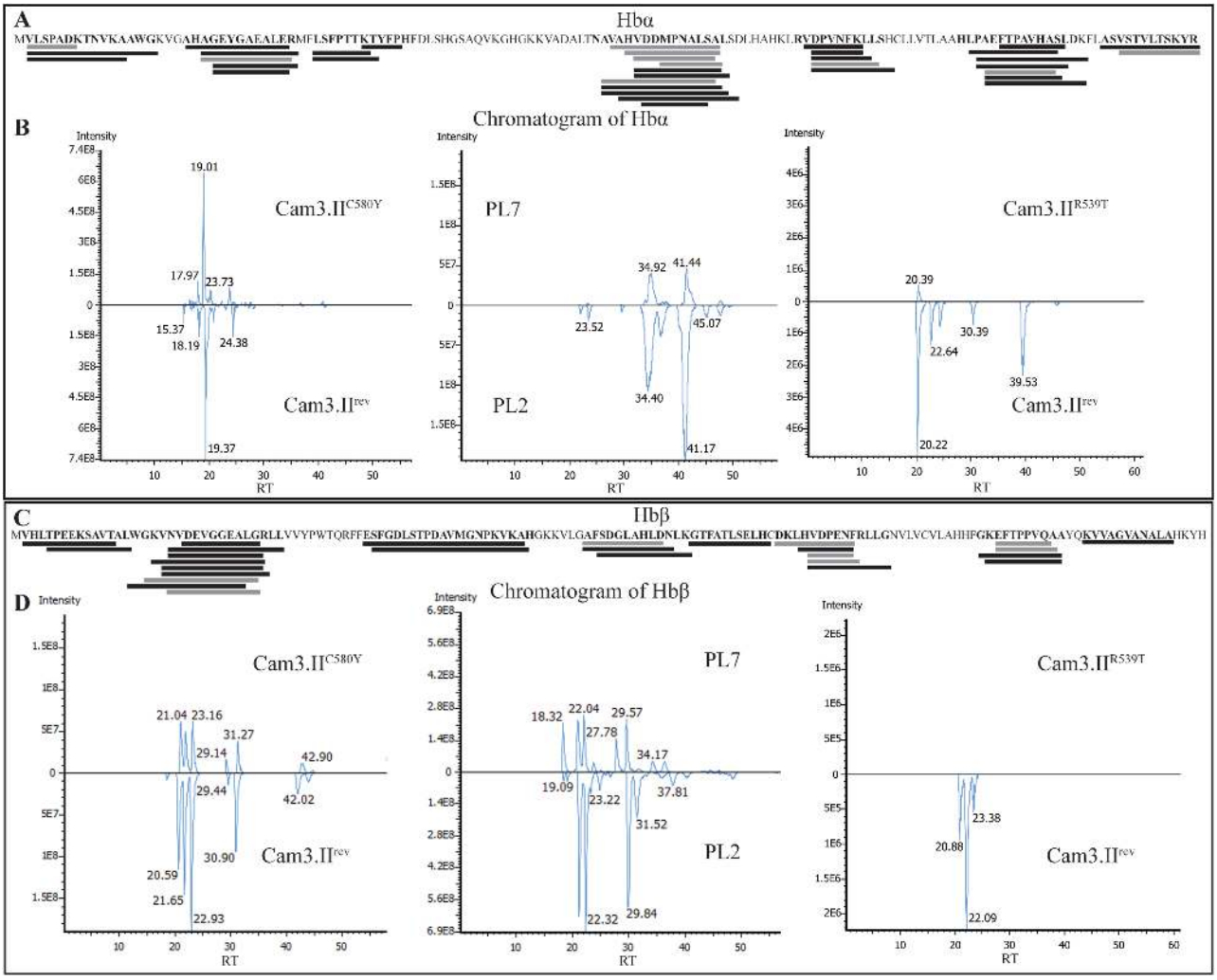

Figure 5. Differentially abundant endogenous peptides originating from hemoglobin (Hb) in artemisinin-resistant versus artemisinin-sensitive lines. *A* and *C,* Sequence coverage of Hbα and Hbβ from peptidomics analysis of resistant lines compared with sensitive lines. The black bars represent endogenous peptides identified that were not significantly different in abundance. The grey bars represent endogenous peptides identified that were significantly decreased in abundance in the resistant lines compared with the sensitive lines. Statistical analysis is shown in Supplementary Data File 3. *B* and *D,* Chromatograms from all detected Hbα and Hbβ peptides in Cam3.II^{C580Y}versus Cam3.II^{rev}, PL7 versus PL2, and Cam3.II^{R539T} versus Cam3.II^{rev}. The chromatograms demonstrated an overview of the decrease in abundance of peptides identified from Hb in the resistant lines (above axis) compared with the sensitive lines (below axis).

Our global peptidomics analysis identified a number of endogenous peptides originating from hemoglobin (alpha and beta subunits) that were decreased in abundance in the resistant lines (Figure 5), suggesting downregulation of hemoglobin uptake or digestion. This decrease in hemoglobin catabolism could result in decreased production of haem, which is necessary to activate artemisinin to mediate parasite killing. Disrupted hemoglobin digestion and endocytosis has previously been demonstrated in artemisinin-resistant rodent parasites [45, 47]. The decreased hemoglobin digestion could be associated with quiescence or a higher proportion of ring-stage parasites in the samples. However, the highly similar proteomics and metabolomics profiles observed here confirmed that all samples were correctly normalized and at the same lifecycle stage at the time of analysis because stage-specific profiles would have been anticipated if significant differences in development were apparent [48]. Dysregulation in the abundance of hemoglobin-derived peptides in chloroquine-resistant *P. falciparum* lines has previously been reported [49]. However, chloroquine resistance was associated with peptide accumulation, and it is therefore unlikely that hemoglobin-derived peptides will provide a sensitive and selective biomarker in the context of multidrug resistance.

In conclusion, through a combined proteomics, metabolomics, and peptidomics analysis, this study revealed the effect of *PfKelch13* mutations on protein expression, metabolic pathways, and endogenous peptide levels in artemisinin-resistant lines compared with their sensitive (*PfKelch13* wild-type) controls. The functional consequences of *PfKelch13* mutations were observed in the form of decreased hemoglobin digestion

and increased glutathione production. The abundance of PfKelch13 protein was 2-fold lower in artemisinin-resistant *PfKelch13* mutants, and reproducible perturbations in the levels of other proteins were not observed. Further validation in field isolates is necessary to determine the potential of PfKelch13 to be developed as a quantitative biomarker for rapid diagnostic testing and monitoring resistance.

Supplementary Data

Supplementary materials are available at *The Journal of Infectious Diseases* online. Consisting of data provided by the authors to benefit the reader, the posted materials are not copyedited and are the sole responsibility of the authors, so questions or comments should be addressed to the corresponding author.

Notes

Acknowledgments. G. S. performed experiments; G. S., A. S., and A. R. analyzed results and made figures; G. S. and D. J. C. designed the research; G. S., A. S., and D. J. C. wrote the manuscript; D. J. C. directed the overall research program. The Australian Red Cross Blood Service in Melbourne is gratefully acknowledged for providing human erythrocytes used for in vitro cultivation of *Plasmodium falciparum* parasites. The authors thank Professor David Fidock for the genetically modified Cambodian isolates and Professor Leann Tilley for field-derived Pailin isolates. Carson Yuan assisted with the data analysis workflow for peptidomics analysis.

Financial support. D. J. C. is funded by a National Health and Medical Research Council Career Development Fellowship (APP1088855)

Potential conflicts of interest. All authors: No reported conflicts. All authors have submitted the ICMJE Form for Disclosure of Potential Conflicts of Interest. Conflicts that the editors consider relevant to the content of the manuscript have been disclosed.

References

1. World Health Organization. World malaria report. Geneva: World Health Organization, **2016**
2. Bhattarai A, Ali AS, Kachur SP, et al. Impact of artemisinin-based combination therapy and insecticide-treated nets on malaria burden in Zanzibar. PLoS Med **2007**; 4:e309.
3. Dondorp AM, Nosten F, Yi P, et al. Artemisinin resistance in *Plasmodium falciparum* malaria. N Engl J Med **2009**; 361:455–67.
4. Witkowski B, Amaratunga C, Khim N, et al. Novel phenotypic assays for the detection of artemisinin-resistant *Plasmodium falciparum* malaria in Cambodia: in-vitro and ex-vivo drug-response studies. Lancet Infect Dis **2013**; 13:1043–9.
5. Witkowski B, Khim N, Chim P, et al. Reduced artemisinin susceptibility of *Plasmodium falciparum* ring stages in western Cambodia. Antimicrob Agents Chemother **2013**; 57:914–23.
6. Ariey F, Witkowski B, Amaratunga C, et al. A molecular marker of artemisinin-resistant *Plasmodium falciparum* malaria. Nature **2014**; 505:50–5.
7. Takala-Harrison S, Jacob CG, Arze C, et al. Independent emergence of artemisinin resistance mutations among *Plasmodium falciparum* in Southeast Asia. J Infect Dis **2015**; 211:670–9.
8. Amaratunga C, Witkowski B, Dek D, et al. *Plasmodium falciparum* founder populations in western Cambodia have reduced artemisinin sensitivity in vitro. Antimicrob Agents Chemother **2014**; 58:4935–7.
9. Liu LY, Yang T, Ji J, et al. Integrating multiple "omics" analyses identifies serological protein biomarkers for preeclampsia. BMC Med **2013**; 11:236.
10. Ashley EA, Dhorda M, Fairhurst RM, et al.; Tracking Resistance to Artemisinin Collaboration (TRAC). Spread of artemisinin resistance in *Plasmodium falciparum* malaria. N Engl J Med **2014**; 371:411–23.
11. Huang F, Takala-Harrison S, Jacob CG, et al. A single mutation in K13 predominates in southern China and is associated with delayed clearance of *Plasmodium falciparum* following artemisinin treatment. J Infect Dis **2015**; 212:1629–35.
12. Amaratunga C, Witkowski B, Khim N, Menard D, Fairhurst RM. Artemisinin resistance in *Plasmodium falciparum*. Lancet Infect Dis **2014**; 14:449–50.
13. Straimer J, Gnädig NF, Witkowski B, et al. Drug resistance. K13-propeller mutations confer artemisinin resistance in *Plasmodium falciparum* clinical isolates. Science **2015**; 347:428–31.
14. Fairhurst RM. Understanding artemisinin-resistant malaria: what a difference a year makes. Curr Opin Infect Dis **2015**; 28:417–25.
15. Taylor SM, Parobek CM, DeConti DK, et al. Absence of putative artemisinin resistance mutations among *Plasmodium falciparum* in Sub-Saharan Africa: a molecular epidemiologic study. J Infect Dis **2015**; 211:680–8.
16. Ngalah BS, Ingasia LA, Cheruiyot AC, et al. Analysis of major genome loci underlying artemisinin resistance and pfmdr1 copy number in pre- and post-ACTs in western Kenya. Sci Rep **2015**; 5:8308.
17. Torrentino-Madamet M, Fall B, Benoit N, et al. Limited polymorphisms in k13 gene in *Plasmodium falciparum* isolates from Dakar, Senegal in 2012–2013. Malar J **2014**; 13:472.
18. Boussaroque A, Fall B, Madamet M, et al. Prevalence of anti-malarial resistance genes in Dakar, Senegal from 2013 to 2014. Malar J **2016**; 15:347.
19. Ménard D, Khim N, Beghain J, et al.; KARMA Consortium. A worldwide map of *Plasmodium falciparum* K13-propeller polymorphisms. N Engl J Med **2016**; 374:2453–64.
20. Roper C, Alifrangis M, Ariey F, et al. Molecular surveillance for artemisinin resistance in Africa. Lancet Infect Dis **2014**; 14:668–70.
21. Ritchie MD, Holzinger ER, Li R, Pendergrass SA, Kim D. Methods of integrating data to uncover genotype-phenotype interactions. Nat Rev Genet **2015**; 16:85–97.
22. Trager W. Cultivation of malaria parasites. Methods Cell Biol **1994**; 45:7–26.
23. Ahn SY, Shin MY, Kim YA, et al. Magnetic separation: a highly effective method for synchronization of cultured erythrocytic *Plasmodium falciparum*. Parasitol Res **2008**; 102:1195–200.
24. Paul F, Roath S, Melville D, Warhurst DC, Osisanya JO. Separation of malaria-infected erythrocytes from whole blood: use of a selective high-gradient magnetic separation technique. Lancet **1981**; 2:70–1.
25. Dogovski C, Xie SC, Burgio G, et al. Targeting the cell stress response of *Plasmodium falciparum* to overcome artemisinin resistance. PLoS Biol **2015**; 13:e1002132.
26. Christophers SR, Fulton JD. Experiments with isolated malaria parasites (*Plasmodium knowlesi*) free from red cells. Ann Trop Med Parasitol **1939**; 33.
27. Boersema PJ, Raijmakers R, Lemeer S, Mohammed S, Heck AJ. Multiplex peptide stable isotope dimethyl labeling for quantitative proteomics. Nat Protoc **2009**; 4:484–94.
28. Rappsilber J, Ishihama Y, Mann M. Stop and go extraction tips for matrix-assisted laser desorption/ionization, nanoelectrospray, and LC/MS sample pretreatment in proteomics. Anal Chem **2003**; 75:663–70.
29. Cox J, Mann M. MaxQuant enables high peptide identification rates, individualized p.p.b.-range mass accuracies and proteome-wide protein quantification. Nat Biotechnol **2008**; 26:1367–72.
30. Dallas DC, Guerrero A, Parker EA, et al. Current peptidomics: applications, purification, identification, quantification, and functional analysis. Proteomics **2015**; 15:1026–38.
31. Hong F, Breitling R, McEntee CW, Wittner BS, Nemhauser JL, Chory J. RankProd: a bioconductor package for detecting differentially expressed genes in meta-analysis. Bioinformatics **2006**; 22:2825–7.
32. Ritchie ME, Phipson B, Wu D, et al. limma powers differential expression analyses for RNA-sequencing and microarray studies. Nucleic Acids Res **2015**; 43:e47.
33. Creek DJ, Chua HH, Cobbold SA, et al. Metabolomics-based screening of the malaria box reveals both novel and established mechanisms of action. Antimicrob Agents Chemother **2016**; 60:6650–63.
34. Stoessel D, Nowell CJ, Jones AJ, et al. Metabolomics and lipidomics reveal perturbation of sphingolipid metabolism by a novel anti-trypanosomal 3-(oxazolo[4,4-b]pyridine-2-yl)anilide. Metabolomics **2016**; 12.
35. Creek DJ, Jankevics A, Breitling R, Watson DG, Barrett MP, Burgess KE. Toward global metabolomics analysis with hydrophilic interaction liquid chromatography-mass spectrometry: improved metabolite identification by retention time prediction. Anal Chem **2011**; 83:8703–10.
36. Creek DJ, Jankevics A, Burgess KE, Breitling R, Barrett MP. IDEOM: an Excel interface for analysis of LC-MS-based metabolomics data. Bioinformatics **2012**; 28:1048–9.
37. Xia J, Sinelnikov IV, Han B, Wishart DS. MetaboAnalyst 3.0—making metabolomics more meaningful. Nucleic Acids Res **2015**; 43:W251–7.
38. Zhang J, Xin L, Shan B, et al. PEAKS DB: de novo sequencing assisted database search for sensitive and accurate peptide identification. Mol Cell Proteomics **2012**; 11:M111.010587.
39. Tilley L, Straimer J, Gnädig NF, Ralph SA, Fidock DA. Artemisinin action and resistance in *Plasmodium falciparum*. Trends Parasitol **2016**; 32:682–96.
40. Adams J, Kelso R, Cooley L. The kelch repeat superfamily of proteins: propellers of cell function. Trends Cell Biol **2000**; 10:17–24.
41. Mok S, Ashley EA, Ferreira PE, et al. Drug resistance. Population transcriptomics of human malaria parasites reveals the mechanism of artemisinin resistance. Science **2015**; 347:431–5.

42. Mbengue A, Bhattacharjee S, Pandharkar T, et al. A molecular mechanism of artemisinin resistance in *Plasmodium falciparum* malaria. Nature **2015**; 520:683–7.
43. Solyakov L, Halbert J, Alam MM, et al. Global kinomic and phospho-proteomic analyses of the human malaria parasite *Plasmodium falciparum*. Nat Commun **2011**; 2:565.
44. Krauth-Siegel RL, Müller JG, Lottspeich F, Schirmer RH. Glutathione reductase and glutamate dehydrogenase of *Plasmodium falciparum*, the causative agent of tropical malaria. Eur J Biochem **1996**; 235:345–50.
45. Witkowski B, Lelièvre J, Nicolau-Travers ML, et al. Evidence for the contribution of the hemozoin synthesis pathway of the murine *Plasmodium yoelii* to the resistance to artemisinin-related drugs. PLoS One **2012**; 7:e32620.
46. Chandra R, Tripathi LM, Saxena JK, Puri SK. Implication of intracellular glutathione and its related enzymes on resistance of malaria parasites to the antimalarial drug arteether. Parasitol Int **2011**; 60:97–100.
47. Henriques G, Martinelli A, Rodrigues L, et al. Artemisinin resistance in rodent malaria—mutation in the AP2 adaptor μ-chain suggests involvement of endocytosis and membrane protein trafficking. Malar J **2013**; 12:118.
48. Olszewski KL, Morrisey JM, Wilinski D, et al. Host–parasite interactions revealed by *Plasmodium falciparum* metabolomics. Cell Host Microbe **2009**; 5:191–9.
49. Lewis IA, Wacker M, Olszewski KL, et al. Metabolic QTL analysis links chloroquine resistance in *Plasmodium falciparum* to impaired hemoglobin catabolism. PLoS Genet **2014**; 10:e1004085.